

# The Journal of Phytopharmacology

(Pharmacognosy and phytomedicine Research)

## Research Article

ISSN 2320-480X

JPHYTO 2023; 12(6): 411-420

November- December

Received: 02-10-2023

Accepted: 24-12-2023

©2023, All rights reserved

doi: 10.31254/phyto.2023.12607

### Ololade Zacchaeus S

Department of Chemistry, Medicinal and Organic Chemistry Unit, University of Medical Sciences, Ondo, Nigeria

### Lajide Labunmi

Department of Chemistry, Medicinal and Organic Chemistry Unit, University of Medical Sciences, Ondo, Nigeria

### Onifade Olayinka F

Department of Chemical Sciences, Biochemistry Unit, Bells University of Technology, Ota, Nigeria

### Eze John C

Department of Chemistry, Medicinal and Organic Chemistry Unit, University of Medical Sciences, Ondo, Nigeria

### Tommy Bessie E

Department of Chemistry, Medicinal and Organic Chemistry Unit, University of Medical Sciences, Ondo, Nigeria

### Orodepo Gabriel O

Department of Chemistry, Medicinal and Organic Chemistry Unit, University of Medical Sciences, Ondo, Nigeria

### Idowu Olaniyi O

Department of Chemistry, Medicinal and Organic Chemistry Unit, University of Medical Sciences, Ondo, Nigeria

### Oyebanji Olawumi T

Department of Chemistry, Medicinal and Organic Chemistry Unit, University of Medical Sciences, Ondo, Nigeria

### Olaniran Anikeola C

Department of Chemistry, Medicinal and Organic Chemistry Unit, University of Medical Sciences, Ondo, Nigeria

## Correspondence:

### Dr. Ololade Zacchaeus S

Department of Chemistry, Medicinal and Organic Chemistry Unit, University of Medical Sciences, Ondo, Nigeria  
Email: [sololade@unimed.edu.ng](mailto:sololade@unimed.edu.ng)

## Exploration of Secondary Metabolites in Flower-Petal *Annona muricata* as Agonists for Peroxisome Proliferator-Activated Receptor-Alpha (PPAR $\alpha$ ) for Liver Function

Ololade Zacchaeus S, Lajide Labunmi, Onifade Olayinka F, Eze John C, Tommy Bessie E, Orodepo Gabriel O, Idowu Olaniyi O, Oyebanji Olawumi T, Olaniran Anikeola C

## ABSTRACT

The expression of PPAR $\alpha$  in the liver is significantly increased in both non-alcoholic fatty liver disease (NAFLD) patients and experimental models. Animal studies have shown promising outcomes in improving histological conditions, such as fibrosis, through the use of PPAR $\alpha$  agonists. This particular petal to act as agonists for PPAR $\alpha$ . Molecular docking and Prime MM-GBSA (Molecular Mechanics-Generalized Born Surface Area) were employed to analyze the ligand binding affinity, atomistic interactions, and protein stability. Additionally, we conducted evaluations of the identified PPAR $\alpha$  agonist candidates to assess their toxicity and pharmacological profiles were conducted. The hit compounds exhibit favourable binding affinity and thermodynamics stability, and interact effectively with key residues in the binding site. Furthermore, the safety assessment indicates minimal to non-acute toxicity and favourable drug-like properties for these compounds. Secondary metabolites in the extract are potential drug candidate. They demonstrate drug-like properties as they adhere to the Lipinski rule.

**Keywords:** *Annona muricata*, Flower-petal, Phytochemicals, PPAR $\alpha$ , ADMET, Liver function, Lipinski rule.

## INTRODUCTION

Natural products from medicinal plants are good sources for deriving phytochemical for drug development [1-3]. Phytochemicals have been produced in the various environment, which represents an alternative resource for new drugs used to treat diseases [4-6]. Natural products remain as a leading source for the development of pharmaceuticals [6-8]. *Annona muricata* (sour sop) is a medicinal plant known as a natural multipurpose phytotherapy agent [9,10]. *A. muricata* is locally used to treat mesenteric lymphadenitis, gastrointestinal disorders, fever, rheumatoid, gouty, joints pain, skin ailments, tuberculosis, nausea, neurological disorders, bacterial and fungal infections, respiratory illnesses, diabetes, parasites and so on [10,11]. Peroxisome proliferator-activated receptor (PPAR)  $\alpha$ ,  $\beta/\delta$ , and  $\gamma$  modulate lipid homeostasis. PPAR $\alpha$  Peroxisome proliferator-activated receptor- $\alpha$  (PPAR $\alpha$ ) is a nuclear hormone receptor which regulates the oxidation and transport of fatty acids. Upon activation it binds as a heterodimer with retinoid X receptor (RXR) to peroxisome response elements in genes involved in fatty acid oxidation. PPAR $\alpha/\gamma$  activation might decrease the hepatic lipid accumulation, oxidative stress and inflammatory cytokine production [12-14]. Peroxisome proliferator-activated receptor (PPAR)  $\alpha$ ,  $\beta/\delta$ , and  $\gamma$  modulate lipid homeostasis. In liver, PPAR $\alpha$  regulates lipid metabolism in the liver, the organ that largely controls whole-body nutrient/energy homeostasis, and its abnormalities may lead to hepatic steatosis, steatohepatitis, steatofibrosis, and liver cancer [15-17]. To the best of our knowledge, there is paucity information on the use of phytochemicals as agonists for peroxisome proliferator-activated receptor-alpha (PPAR $\alpha$ ) so far. This study assessed their agonistic properties by comparing their binding affinity, binding interactions, and binding energy to a known agonist, fenofibrate and saroglitazar. Therefore, the research showcased the exploration of secondary metabolites in flower-petal extract of *A. muricata* as agonists for peroxisome proliferator-activated receptor-alpha (PPAR $\alpha$ ) for liver function.

## MATERIALS AND METHODS

### Protein retrieval and preparation

The 3D crystal structure of Peroxisome proliferator-activated receptor alpha (PPAR $\alpha$ ) was obtained from the Protein Data Bank (PDB ID = 2ZNN) via their website (<http://www.rcsb.org/pdb>). The protein was prepared and visualized using the Protein Preparation Wizard panel in the Schrödinger Maestro suite 11.5 [18]. The preparation involved filling in missing loops and side chains using Prime, establishing

extrinsic hydrogen bonds, assigning bond orders, forming disulfide bonds, adjusting the pH to  $7.0 \pm 2.0$  with Epik<sup>[19]</sup>, and removing water and other molecules used in the crystallization process. Further optimization of the protein was performed using PROPKA at pH 7.0, followed by restrained minimization employing the OPLS3 force field with unconstrained hydrogen atoms and restrained heavy<sup>[20]</sup>, thus completing the protein preparation steps.

### Ligand preparation

The PPAR $\alpha$  agonist structures, Fenofibrate and Saroglitazar<sup>[21,22]</sup>, and sixty (60) phytochemicals from the *Annona muricata* flower were downloaded from the NCBI PubChem database (<https://pubchem.ncbi.nlm.nih.gov>) in sdf format. Using the LigPrep interface<sup>[23]</sup>, the 2D structures were transformed into optimized 3D structures. Ligand preparation involved desalting, tautomer generation, and the creation of low-energy conformations using the OPLS3 force field<sup>[20]</sup>. Epik was used to generate ionization states at pH  $7.0 \pm 2.0$ <sup>[19]</sup>.

### Receptor grid generation

A grid box was created to encompass the PPAR $\alpha$  ligand binding site using the Glide Grid Generation panel in Schrödinger Maestro 11.5<sup>[24]</sup>. The coordinates of the PPAR $\alpha$  co-crystallized ligand served as the centre for the grid, with X, Y, and Z dimensions set at 10.96, 4.68, and -8.28, respectively. The nonpolar receptor atoms were assigned a van der Waals (vdW) radius scaling factor of 1.0 Å, and a partial atomic charge of 0.25 was applied. This setup provided the necessary site for ligand docking within the PPAR $\alpha$  binding site.

### Molecular docking

The prepared compounds were docked into the PPAR $\alpha$  ligand binding site using the generated grid and the Ligand docking panel of the Glide tool in Schrödinger Maestro 11.5 (Figure 1). The docking process involved two steps: Standard Precision (SP) docking with flexible ligand sampling, followed by Extra Precision (XP) docking of the top 33% ranked compounds<sup>[24]</sup>. The default values were used for the partial charge cutoff (0.15) and van der Waals radii scaling factors (0.80). Additionally, the co-crystallized ligand was also subjected to docking.

### Molecular docking validation

The PPAR $\alpha$  agonist, originally co-crystallized with the protein, was extracted and docked into the PPAR $\alpha$  ligand binding site. To validate the docking procedure, the Root Mean Square Deviation (RMSD)<sup>[25]</sup> between the docked poses and the native PDB pose was calculated. The RMSD calculation used the "Compute RMSD to input ligand geometries" option in the output interface of the Ligand docking's glide tool. This provided a measure of the similarity between the docked poses and the original PDB pose<sup>[23,26]</sup>.

### Prime MM-GBSA

The pose file for the docked ligand- PPAR $\alpha$  complexes was used to calculate the binding free energy ( $\Delta G_{\text{bind}}$ ) between the docked ligands and PPAR $\alpha$  ligand binding site using Molecular Mechanics-Generalized Born Surface Area (MM-GBSA) panel of the Prime tool of Schrodinger 11.5. The OPLS3 force field, the VSGB continuum solvation model, and the minimize sampling-method options were used<sup>[27-29]</sup>.

### Pharmacokinetics

SwissADME (<http://www.swissadme.ch/>) and ProTox (<https://tox-new.charite.de/protoxII/>) web tools were employed to evaluate the pharmacokinetics, drug-likeness, and toxicity features (ADMET) of the hit compounds and reference ligands. The ligands' canonical SMILES were uploaded to both servers<sup>[30,31]</sup>, generating the relevant ADMET parameters automatically. This analysis provided insights into the compounds' pharmacokinetic properties, drug-likeness, and potential toxicity.

## RESULTS AND DISCUSSION

### Molecular Docking

The phytochemicals extracted from the *Annona muricata* flower demonstrate potential as agonists for PPAR $\alpha$ . This study assessed their agonistic properties by comparing their binding affinity, binding interactions, and binding energy to a known agonist, Fenofibrate and Saroglitazar. The binding affinity was evaluated using molecular docking, wherein the docking score corresponds to the binding affinity. A more negative docking score indicates a stronger binding affinity<sup>[32]</sup>. The docking score of our top scoring compound and the reference ligand is shown in Table 1. The top scoring compounds maltose, methyl 4,6-O-nonylidene-alpha-D-glucopyranoside, 1-heptadec-1-ynyl-cyclopentanol, alpha-l-rhamnopyranose, 1-(2-deoxy-alpha-D-erythro-pentofuranosyl)-thymine,  $\beta$ -eudesm-4(14)-en-11-ol are represented as the C1, C2, C3, C4, C5, and C6 respectively, in this context. C1, C2, C3, C4, C5, and C6 show the docking score of -9.467 Kcal/mol, -8.346 Kcal/mol, -8.026 Kcal/mol, -7.602 Kcal/mol, -7.423 Kcal/mol, and -6.603 Kcal/mol respectively. And the reference ligand, Fenofibrate and Saroglitazar score -8.009 Kcal/mol and -7.852 Kcal/mol respectively. The higher and close docking score of our hit compounds compared to the reference ligand shows they can bind with better and similar strength with PPAR $\alpha$ . Thus, revealing their agonistic potential on PPAR $\alpha$ . We further validate the docking procedure to test its reliability by computing the RMSD between the docked co-ligand pose and the native PDB pose (Figure 2). An RMSD value  $\leq 2.0$  Å indicates accurate docking<sup>[26,33]</sup>. Our analysis resulted in an RMSD of 0.360 Å, confirming our docking protocol is validity and reliable, and proving the accuracy of our results. It is also important to understand the binding interaction that exist between the ligand and the protein to identify key regions of the target molecule that participate in binding, providing guide for optimization, and predict potential efficacy<sup>[34]</sup>. The binding interaction of our top-ranked compounds and the reference ligand with specific residues in the PPAR $\alpha$  binding pocket is shown in Table 1. The ligands establish hydrogen bonds, polar interactions, hydrophobic interactions, and  $\pi$ - $\pi$  stacking interactions with critical residues, including Asn 219, Thr 279, Ser 280, Thr 283, Tyr 314, Leu 331, Ala 333, Tyr 334, Gly 335, His 440, and Tyr 464 (Oyama *et al*, 2009; Bernardes *et al*, 2013). Notably, the hydrogen bond involving Tyr 464 maintains the protein's active conformation, and Tyr 314 contributes to PPAR $\alpha$  selectivity<sup>[35]</sup>. Our top ligands effectively interact with these residues. Specifically, C1 interacts with Asn 219, Tyr 334, and Thr 283; C2 interacts with Asn 219, Thr 279, and Thr 283; C3 predominantly engages in hydrophobic interactions; C4 interacts with Ser 280, His 440, and Tyr 464; C5 interacts with Ala 333, and C6 interacts with Ser 280, His 440, and Tyr 464. Furthermore, Fenofibrate interacts with Thr 279, and Saroglitazar interacts with Tyr 334 and His 440. As shown in Figure 3 for the 2D interaction diagram, these findings further validate the potential of these *Annona muricata*

phytoconstituents as PPAR $\alpha$  agonists. In fact, it was reported the ameliorative effect of this plant on hepatic lipid metabolism through AMPK/PPAR $\alpha$  pathway in diabetic mice [36].

### Binding Energy using MMGBSA

MM-GBSA (Molecular Mechanics-Generalized Born Surface Area) measures the thermodynamic stability of the ligand-receptor interaction by calculating the change in binding free energy ( $\Delta G_{\text{bind}}$ ) [27,37]. Negative  $\Delta G_{\text{bind}}$  indicates favorable binding, indicating stronger ligand affinity for the target receptor in the bound state than in the unbound state. The more negative the score, the better the ligand stability in the binding site of protein [28,29,38]. The result of this procedure is shown in Figure 3. C1, C2, C3, C4, C5, and C6 score -31.73  $\Delta G_{\text{bind}}$ , -44.65  $\Delta G_{\text{bind}}$ , -66.44  $\Delta G_{\text{bind}}$ , -30.95  $\Delta G_{\text{bind}}$ , -43.95  $\Delta G_{\text{bind}}$ , and -37.12  $\Delta G_{\text{bind}}$  respectively; and the reference ligands score -49.63  $\Delta G_{\text{bind}}$  (Fenofibrate), and -58.64  $\Delta G_{\text{bind}}$  (Saroglitazar). This result is shown in Table 1. The negative  $\Delta G_{\text{bind}}$  indicates favorable binding between the ligand and the receptor; and the close score compared to the reference ligands reveal they stable in the PPAR $\alpha$  ligand binding site. Thus, further supporting the agonistic potential of the *A. muricata* phytochemicals.

### ADMET and the drug-likeness predictions.

The considerable rate of unsuccessful drug candidates in advanced stages of development is often attributed to deficiencies in absorption, distribution, metabolism, excretion, and toxicity (ADME/Tox). Consequently, computational techniques have emerged as a rapid and cost-efficient means of screening therapeutic compounds [32]. Herein, we screen our top-ranking compounds to predict their ADME/Tox properties. The compounds maltose, methyl 4,6-O-nonylidene- $\alpha$ -D-glucopyranoside, 1-heptadec-1-ynyl-cyclopentanol,  $\alpha$ -l-rhamnopyranose, 1-(2-deoxy- $\alpha$ -D-erythro-pentofuranosyl)-thymine, and Beta-eudesm-4(14)-en-11-ol are denoted as C1, C2, C3, C4, C5, and C6, respectively, based on their top scores. The compounds' absorption and distribution properties were assessed (Table 2). All compounds, except C1 and C3, exhibited high gastrointestinal absorption, indicating their effective uptake into the bloodstream after oral administration [39]. Furthermore, with the exception of C1 and C4, none of the compounds acted as substrates for P-Glycoprotein, an efflux protein that prevents them from reaching their target [40-42].

Regarding blood-brain barrier permeability, only Fenofibrate and C6 did not demonstrate the ability to cross the barrier. And reports has been shown that Fenofibrate is not BBB permeant [43], thus supporting the our findings. Compounds that can permeate the BBB have ability to cross the bloodstream and enter the brain tissue where they interact with different targets in the central nervous system (CNS) and exert effects ranging from therapeutics to potential toxicity [44-47]. Overall, further research is needed to clarify the specific roles of these compounds in the brain. In terms of drug metabolism properties, only

C3 and C4 inhibits one of the CYP450 enzyme, while the remaining compounds showed no inhibition at all. The reference ligands inhibited four out of the five CYP450 enzymes (Table 2). The inhibition of CYP450 enzymes can result in drug-drug interactions, leading to changes in plasma concentration, half-life, and possibly increasing the risk of toxicity [48-50]. The absence of inhibitory effects suggests favorable compound metabolism, and excretion from the body. Conversely, inhibition indicate potential challenges in metabolism, and excretion, which may result in increased compounds half-life but also raise concerns regarding potential toxicity.

All compounds investigated, are potential drug candidate except C1. They demonstrate drug-like properties as they adhere to the Lipinski rule, which states that drug-like compounds should not violate more than one of the following criteria: molecular weight (MW) < 500, hydrogen bond donors (HBD) < 5, hydrogen bond acceptors (HBA) < 10, and LogP  $\leq$  5 [51-53] as shown the results in Table 3. Compounds with a polar surface area (PSA) greater than 140  $\text{\AA}^2$  exhibit reduced oral bioavailability and cell membrane permeability [52,54-55]. Only C1 exceeds this threshold with a value of 189.53  $\text{\AA}^2$ , while the others, including the reference ligand, have scores ranging from 20.23  $\text{\AA}^2$  to 104.55  $\text{\AA}^2$ , indicating their availability in the system. Furthermore, a bioavailability score of 0.55 or higher suggests the compounds' availability in the system [56].

ProTox was used predict the acute toxicity, hepatotoxicity, carcinogenicity, immunotoxicity, mutagenicity, cytotoxicity of the studied compounds. The toxicity prediction results is shown in Table 4. The results were predicted with good accuracy (>50%) for most compounds, except for C5 with a poor prediction accuracy of 12%. Fenofibrate was predicted to be carcinogenic that is, it can induce tumours or increase the incidence of tumours, however, studies have shown the opposite [15, 57-58], the reason for this prediction is unknown; and C2 can have adverse effect on the immune system, it is immunotoxin. The "toxicity class" reflects acute toxicity. And, the LD<sub>50</sub> value represents the dose predicted to kill 50% of a population [59]. Acute toxicity generally increases with decreasing LD<sub>50</sub> [60]. Toxicity Class 1 is fatal if swallowed (LD<sub>50</sub>  $\leq$  5 mg/Kg); Class 2 is fatal if swallowed (5 mg/Kg < LD<sub>50</sub>  $\leq$  50 mg/Kg); Class 3 is toxic if swallowed (50 mg/Kg < LD<sub>50</sub>  $\leq$  300 mg/Kg); Class 4 is harmful if swallowed (300 mg/Kg < LD<sub>50</sub>  $\leq$  2000 mg/Kg); Class 5 may be harmful if swallowed (2000 mg/Kg < LD<sub>50</sub>  $\leq$  5000 mg/Kg); Class 6 is not harmful [61]. Thus, C4 and C6, with LD<sub>50</sub> values  $\geq$  10000, is not harmful; C1 with a toxicity class 3 and an LD<sub>50</sub> of 51 mg/kg is predicted toxic; and C2, C3, C6 and the reference ligands with LD<sub>50</sub> values ranging from 475-2000mg/kg are predicted harmful. The Log *k<sub>p</sub>* value, which represents the skin permeation coefficient in Table 2, provides insight into the compounds' ability to penetrate the skin and induce toxicity. Negative Log *k<sub>p</sub>* values suggest limited skin penetration, with a greater negative value indicating reduced permeation potential [26,62,63]. In our study, the compounds exhibited negative Log *k<sub>p</sub>* values ranging from -10.92 cm/s to -2.08 cm/s, signifying their inability to permeate the skin and cause toxicity.

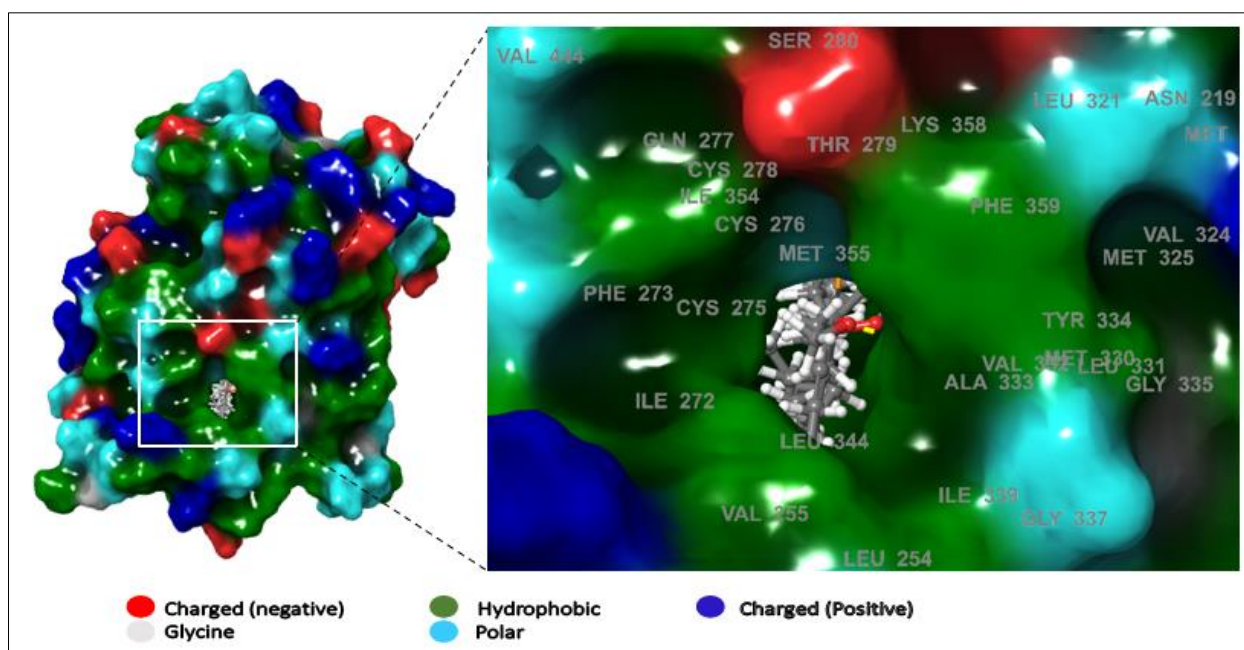


**Figure 1:** The 3D view of the Peroxisome proliferator activated receptor alpha (PPARα) showing the bound ligands, and the site residues. The legend shows the Residue property

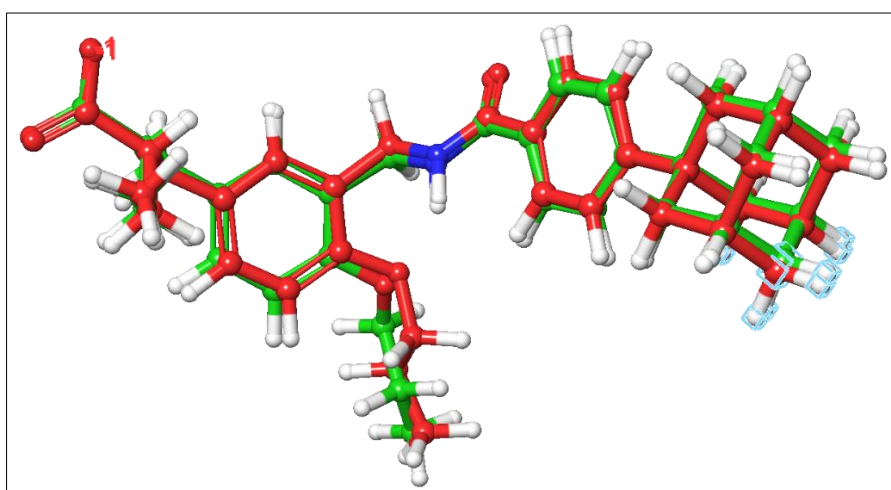
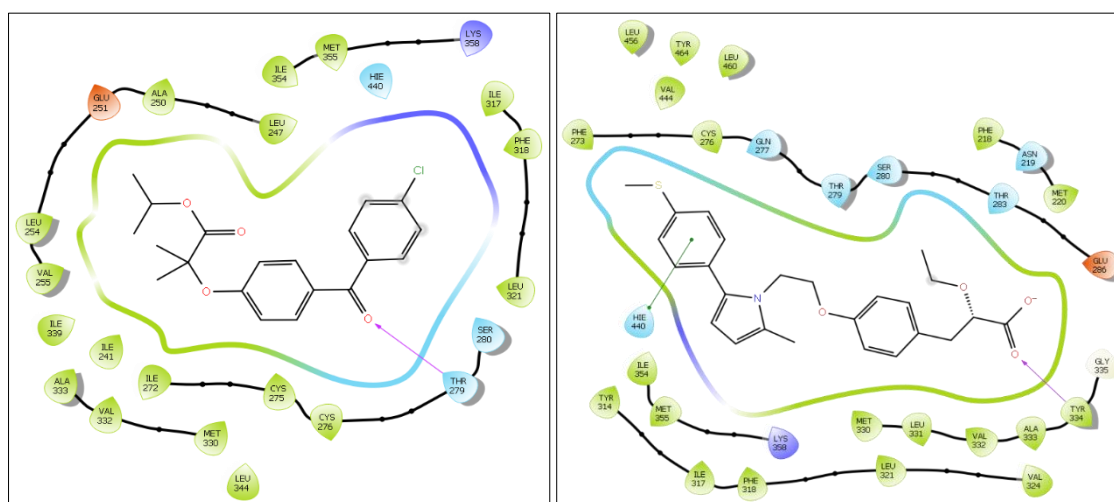


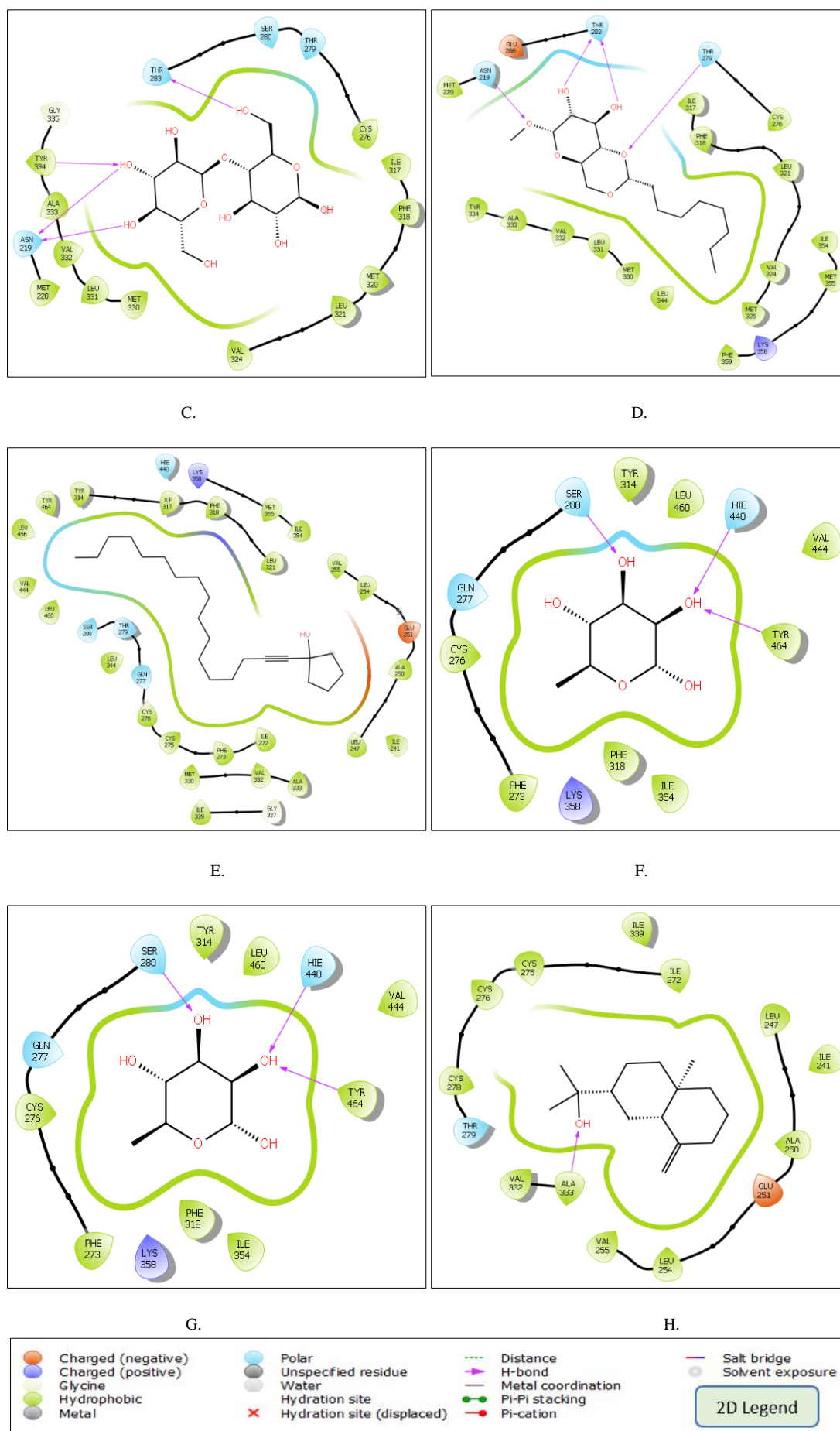
**Figure 2:** The superimposition of the native co-ligand poses and the docked co-ligand pose on PPARα (RMSD is 0.360Å). Red is docked pose, Green is native PDB pose.



A.

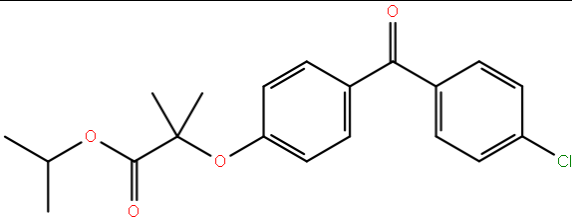
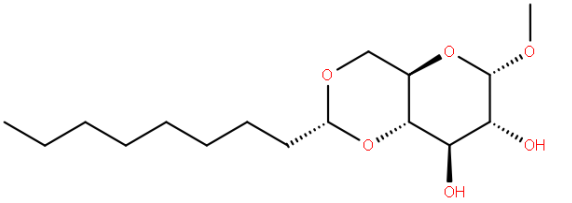
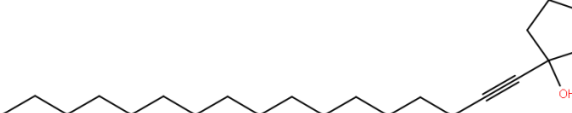
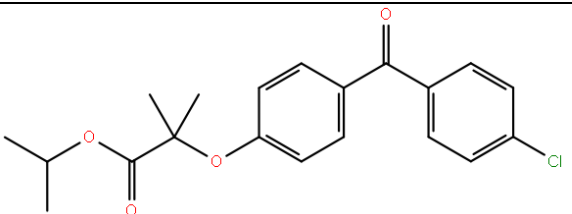
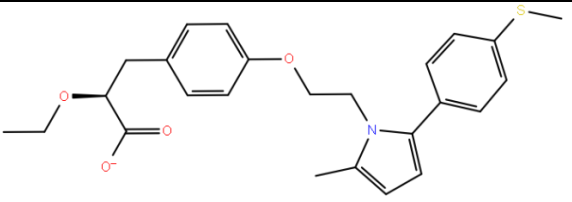
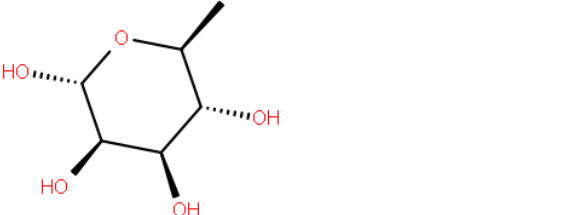
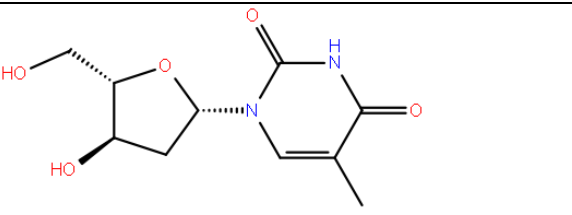
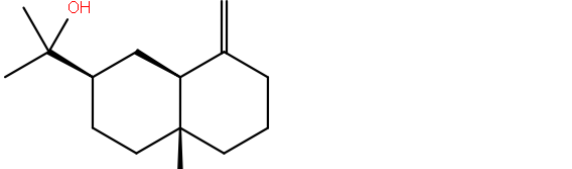
B.





**Figure 3:** The 2D interaction diagram of the top hit ligands and reference ligands in the active site of PPAR $\alpha$  with their interaction legend. (a) Fenofibrate, (b) Saroglitazar, (c) C1, (d) C2, (e) C3, (f) C4, (g) C5, (h) C6.

**Table 1:** 2D structure, docking score, and PPAR $\alpha$  residues-ligand interaction of the top six (6) ranking compounds from *Annona muricata* flower-Petal and reference ligands

Active compounds	2D Structures	Docking scores (kcal/mol)	MMGBSA dG Bind	H-bond and <i>PI-PI</i> stacking with PPAR $\alpha$
C1		-9.467	-31.73	Asn 219 Tyr 334 Thr 283
C2		-8.346	-44.65	Asn 219 Thr 279 Thr 283
C3		-8.026	-66.44	-
Fenofibrate¶		-8.009	-49.63	Thr 279
Saroglitazar¶		-7.852	-58.64	Tyr 334 <i>His 440</i>
C4		-7.602	-30.95	Ser 280 His 440 Tyr 464
C5		-7.423	-43.95	Ser 280 <i>His 440</i>
C6		-6.603	-37.12	Ala 333

¶The reference ligands. C1 = Maltose, C2 = Methyl 4,6-O-nonylidene-alpha-D-glucopyranoside, C3 = 1-heptadec-1-ynyl-cyclopentanol, C4 = Alpha-l-rhamnopyranose, C5 = 1-(2-deoxy-alpha-D-erythro-pentofuranosyl)-thymine, C6 = Beta-eudesm-4(14)-en-11-ol.

**Table 2:** Prediction of the Pharmacokinetic Properties of the Hit Compounds and the reference ligand by Swiss ADME

Compounds	GI abs	BBB Perm	P-gp sub	CYP1A2 inhibitor*	CYP2C19 inhibitor*	CYP2C9 inhibitor*	CYP2D6 inhibitor*	CYP3A4 inhibitor*	Log <i>k<sub>p</sub></i> (cm/s)
Fenofibrate¶	High	+	-	+	+	+	+	-	-4.83
Saroglitazar¶	High	-	-	-	+	+	+	+	-5.47
C1	Low	-	+	-	-	-	-	-	-10.92
C2	High	-	-	-	-	-	-	-	-6.56
C3	Low	-	-	+	-	-	-	-	-2.08
C4	High	-	+	-	-	-	-	-	-8.79
C5	High	-	-	-	-	-	-	-	-8.61
C6	High	+	-	-	-	+	-	-	-4.85

¶The reference ligands. + denotes Yes, - denotes No. GI abs- gastrointestinal absorption. BBB perm- Blood-brain barrier permeant. P-gp sub- P-Glycoprotein substrate. \*Cytochrome p450 enzyme isoforms inhibition. Log *k<sub>p</sub>* -Skin permeation.

**Table 3:** Prediction of the Drug Likeness Properties of the Pit Compounds and the Reference Ligand by SwissADME

Compounds	MW (g/mol)	HBD	HBA	TPSA (Å <sup>2</sup> )	C. Logp	Bio. Sco.	Lipinski violation
Fenofibrate¶	360.83	0	4	52.6	4.4	0.55	0
Saroglitazar¶	439.57	1	4	85.99	4.4	0.56	0
C1	342.3	8	11	189.53	-3.39	0.17	2
C2	318.41	2	6	77.38	1.92	0.55	0
C3	320.55	1	1	20.23	6.75	0.55	1
C4	164.16	4	5	90.15	-1.46	0.55	0
C5	242.23	3	5	104.55	-0.61	0.55	0
C6	222.37	1	1	20.23	3.61	0.55	0

¶The reference ligands. C1 = Maltose, C2 = Methyl 4,6-O-nonylidene-alpha-D-glucopyranoside, C3 = 1-heptadec-1-ynyl-cyclopentanol, C4 = Alpha-l-rhamnopyranose, C5= 1-(2-deoxy-alpha-D-erythro-pentofuranosyl)-thymine, C6 = Beta-eudesm-4(14)-en-11-ol.

**Table 4:** ProTox Toxicity Prediction of the Hit Compounds and the Reference Ligand

Compounds	HT	CG	IT	MG	CT	Toxicity class*	PA (%)	LD <sub>50</sub> (mg/kg)
Fenofibrate¶	-	+	-	-	-	4	100	1600
Saroglitazar¶	-	-	-	-	-	4	54.26	475
C1	-	-	-	-	-	3	100	51
C2	-	-	+	-	-	4	72.9	2000
C3	-	-	-	-	-	4	69.26	825
C4	-	-	-	-	-	6	67.38	23000
C5	-	-	-	-	-	6	12	10000
C6	-	-	-	-	-	4	100	2000

¶The reference ligands. + denotes active, - denotes inactive. HT-Hepatotoxicity, CG-Cytogenicity, IT-Immunotoxicity, MG-Mutagenicity, CT-Cytogenicity, PA-Prediction Accuracy. \*If swallowed, Class 1 is fatal, Class 2 is fatal, Class 3 is toxic, Class 4 is harmful, Class 5 may be harmful, and Class 6 is not harmful.

## CONCLUSION

These findings showed that some phytochemicals in the flower-petal of *A. muricata* hold promise as potential PPAR $\alpha$  agonists. Almost all compounds investigated, are potential drug candidate. They demonstrate drug-like properties as they adhere to the Lipinski rule. The negative  $\Delta G_{bind}$  indicates favorable binding between the ligand and the receptor; and the close score compared to the reference ligands reveal they stable in the PPAR $\alpha$  ligand binding site. Thus, further supporting the agonistic potential of the *A. muricata* phytochemicals.

**Conflict of interest:** We have no conflict of interest.

## REFERENCES

1. Veeresham C. Natural products derived from plants as a source of drugs. J Adv Pharm Technol Res. 2012, 3(4):200-1. 3(4): 200–201, doi: 10.4103/2231-4040.104709.
2. Thomford NE, Senthebane DA, Rowe A, Munro D, Seele P, Maroyi A, Dzobo K. Natural Products for Drug Discovery in the 21st Century: Innovations for Novel Drug Discovery. International Journal of Molecular Sciences. 2018; 19(6):1578. <https://doi.org/10.3390/ijms19061578>.

3. Gbenga-Fabusiwa FJ, Jeff-Agboola YA, Ololade ZS, Akinrinmade R, Agbaje DO. Waste-to-wealth; nutritional potential of five selected fruit peels and their health benefits: A review. *African Journal of Food Science*, 2022, 16(7), 172-183.
4. Lu WY, Li HJ, Li QY, Wu YC. Application of marine natural products in drug research. *Bioorg Med Chem.*, 2021, 35:116058. doi: 10.1016/j.bmc.2021.116058.
5. Alao FO, Ololade ZS, Garba JO. Solvent Polarity and Temperature Effects on Extracted Secondary Metabolite from the Fruit of *Tetrapleura tetraptera* and its Antibacterial Potential on Uropathogens, *Global Journal of Medical Research Microbiology and Pathology*, 2022, 22(1), 23-31.
6. Adesina AR, Kajihausa OE, Sobukola OP, Ololade ZS. Some Quality Attributes of Gluten Free Fried Products from Defatted Peanut Flour and Starches of Common Tropical Roots. *International Journal of Agricultural Science and Food Technology*, 2022a, 8(4), 265-272.
7. Ololade ZS, Abiose MM. Analyses of the Secondary Metabolites, Radical Scavenging, Protein Denaturation and Antibacterial Activities of the Stem Extract of *Annona squamosa*, *Nigerian Journal of Science*, 2019, 53(1), 39-54.
8. Adesina AR, Kajihausa OE, Sobukola OP, Ololade ZS. Some Quality Attributes of Gluten Free Fried Products from Defatted Peanut Flour and Starches of Common Tropical Roots, *International Journal of Agricultural Science and Food Technology*, 2022b, 8(4), 265-272.
9. Pai BM, Rajesh G, Shenoy R, Rao A. Anti-microbial Efficacy of Soursop Leaf Extract (*Annona muricata*) on Oral Pathogens: An In-vitro Study. *J Clin Diagn Res.*, 2016, 10(11):ZC01-ZC04. doi: 10.7860/JCDR/2016/18329.8762.
10. Ololade ZS, Fakankun OA, Alao FO, Ajewole OO. Free Radical Scavenging, Antioxidant and Antibacterial Activities of the Fruit-Pulp Essential Oil of *Annona muricata* and Its Phytochemical Composition, *International Journal of Applied Research and Technology*. 2016, 5 (2), 47-52.
11. Mutakin M, Fauziati R, Fadhilah FN, Zuhrotun A, Amalia R, Hadisaputri YE. Pharmacological Activities of Soursop (*Annona muricata* Lin.). *Molecules*, 2022, 27(4):1201. doi: 10.3390/molecules27041201.
12. Kersten S, Seydoux J, Peters JM, Gonzalez FJ, Desvergne B, Wahli W. Peroxisome proliferator-activated receptor alpha mediates the adaptive response to fasting. *J Clin Invest.*, 1999, 103(11):1489-98. doi: 10.1172/JCI6223.
13. Tyagi S, Gupta P, Saini AS, Kaushal C, Sharma S. The peroxisome proliferator-activated receptor: A family of nuclear receptors role in various diseases. *J Adv Pharm Technol Res.*, 2011, 2(4):236-40. doi: 10.4103/2231-4040.90879.
14. Grygiel-Górniak B. Peroxisome proliferator-activated receptors and their ligands: nutritional and clinical implications - a review. *Nutr J* 2014, 13, 17, <https://doi.org/10.1186/1475-2891-13-17>.
15. Wang Y, Nakajima T, Gonzalez FJ, Tanaka N. PPARs as Metabolic Regulators in the Liver: Lessons from Liver-Specific PPAR-Null Mice. *International Journal of Molecular Sciences*. 2020, 21(6):2061. <https://doi.org/10.3390/ijms21062061>
16. Todisco S, Santarsiero A, Convertini P, De Stefano G, Gilio M, Iacobazzi V, Infantino V. PPAR Alpha as a Metabolic Modulator of the Liver: Role in the Pathogenesis of Nonalcoholic Steatohepatitis (NASH). *Biology (Basel)*. 2022, 11(5):792. doi: 10.3390/biology11050792.
17. Fougerat A, Montagner A, Loiseau N, Guillou H, Wahli W. Peroxisome Proliferator-Activated Receptors and Their Novel Ligands as Candidates for the Treatment of Non-Alcoholic Fatty Liver Disease. *Cells*, 2020, 9 (7), 1-53.
18. Sastry GM, Adzhigirey M, Day T, Annabhimoju R, Sherman W. Protein and ligand preparation: Parameters, protocols, and influence on virtual screening enrichments. *Journal of Computer-Aided Molecular Design*, 2013, 27(3), 221–234. <https://doi.org/10.1007/s10822-013-9644-8>.
19. Shelley JC, Cholleti A, Frye LL, Greenwood JR, Timlin MR, Uchimaya M. Epik: A software program for pK<sub>a</sub> prediction and protonation state generation for drug-like molecules. *Journal of Computer-Aided Molecular Design*, 2007, 21(12), 681–691. <https://doi.org/10.1007/s10822-007-9133-z>
20. Harder E, Damm W, Maple J, Wu C, Reboul M, Xiang JY, Wang L, Lupyan D, Dahlgren MK, Knight JL, Kaus JW, Cerutti DS, Krilov G, Jorgensen WL, Abel R, Friesner RA. OPLS3: A Force Field Providing Broad Coverage of Drug-like Small Molecules and Proteins. *Journal of Chemical Theory and Computation*, 2016, 12(1), 281–296. <https://doi.org/10.1021/acs.jctc.5b00864>
21. Jain MR, Giri SR, Trivedi C, Bhoi B, Rath A, Vanage G, Vyas P, Ranvir R, Patel PR. Saroglitazar, a novel PPAR $\alpha$ / $\gamma$  agonist with predominant PPAR $\alpha$  activity, shows lipid-lowering and insulin-sensitizing effects in preclinical models. *Pharmacology Research & Perspectives*, 2015, 3(3), e00136. <https://doi.org/10.1002/prp2.136>
22. Sidhu G, Tripp J. Fenofibrate. In *StatPearls*. StatPearls Publishing. 2023, <http://www.ncbi.nlm.nih.gov/books/NBK559219/>
23. Schrodinger. What is the difference between Glide core RMSD as set up in the Core tab, and the feature “Compute RMSD to input ligand geometries” in the Output tab? Which should I use? | Schrödinger. 2012, <https://www.schrodinger.com/kb/1682>
24. Friesner RA, Banks JL, Murphy RB, Halgren TA, Klicic JJ, Mainz DT, Repasky MP, Knoll EH, Shelley M, Perry JK, Shaw DE, Francis P, Shenkin PS. Glide: A new approach for rapid, accurate docking and scoring. 1. Method and assessment of docking accuracy. *Journal of Medicinal Chemistry*, 2004, 47(7), 1739–1749. <https://doi.org/10.1021/jm0306430>
25. Kufareva I, Abagyan R. Methods of protein structure comparison. *Methods in Molecular Biology (Clifton, N.J.)*, 2012, 857, 231–257. [https://doi.org/10.1007/978-1-61779-588-6\\_10](https://doi.org/10.1007/978-1-61779-588-6_10)
26. Alade AA, Ahmed SA, Mujwar S, Kikiowo B, Akinnusi PA, Olubode SO, Olufemi OM, Ohilebo AA. Identification of levomenthol derivatives as potential dipeptidyl peptidase-4 inhibitors: A comparative study with gliptins. *Journal of Biomolecular Structure and Dynamics*, 2023, 0(0), 1–19. <https://doi.org/10.1080/07391102.2023.2217927>
27. Kollman PA, Massova I, Reyes C, Kuhn B, Huo S, Chong L, Lee M, Lee T, Duan Y, Wang W, Donini O, Cieplak P, Srinivasan J, Case DA, Cheatham TE. Calculating Structures and Free Energies of Complex Molecules: Combining Molecular Mechanics and Continuum Models. *Accounts of Chemical Research*, 2000, 33(12), 889–897. <https://doi.org/10.1021/ar000033j>



28. Lyne PD, Lamb ML, Saeh JC. Accurate prediction of the relative potencies of members of a series of kinase inhibitors using molecular docking and MM-GBSA scoring. *Journal of Medicinal Chemistry*, 2006, 49(16), 4805–4808. <https://doi.org/10.1021/jm060522a>
29. Hayes JM, Archontis G. MM-GB(PB)SA Calculations of Protein-Ligand Binding Free Energies. In *Molecular Dynamics—Studies of Synthetic and Biological Macromolecules*. IntechOpen. 2012, <https://doi.org/10.5772/37107>
30. Daina A, Michielin O, Zoete V. SwissADME: A free web tool to evaluate pharmacokinetics, drug-likeness and medicinal chemistry friendliness of small molecules. *Scientific Reports*, 2017, 7, 42717. <https://doi.org/10.1038/srep42717>
31. Banerjee P, Eckert AO, Schrey AK, Preissner R. ProTox-II: A webserver for the prediction of toxicity of chemicals. *Nucleic Acids Research*, 2018, 46(W1), W257–W263. <https://doi.org/10.1093/nar/gky318>
32. Omoboyowa DA, Balogun TA, Omomule OM, Saibu OA. Identification of Terpenoids From *Abrus precatorius* Against Parkinson's Disease Proteins Using In Silico Approach. *Bioinformatics and Biology Insights*, 2021, 15, 11779322211050756. <https://doi.org/10.1177/11779322211050757>
33. Livingstone DJ, Davis AM. *Drug Design Strategies: Quantitative Approaches*. Royal Society of Chemistry. 2011.
34. Fu Y, Zhao J, Chen Z. Insights into the Molecular Mechanisms of Protein-Ligand Interactions by Molecular Docking and Molecular Dynamics Simulation: A Case of Oligopeptide Binding Protein. *Computational and Mathematical Methods in Medicine*, 2018, 3502514. <https://doi.org/10.1155/2018/3502514>
35. Bernardes A, Souza PCT, Muniz JRC, Ricci CG, Ayers SD, Parekh NM, Godoy AS, Trivella DBB, Reinach P, Webb P, Skaf MS, Polikarpov I. Molecular Mechanism of Peroxisome Proliferator-Activated Receptor  $\alpha$  Activation by WY14643: A New Mode of Ligand Recognition and Receptor Stabilization. *Journal of Molecular Biology*, 2013, 425(16), 2878–2893. <https://doi.org/10.1016/j.jmb.2013.05.010>
36. Son Y, Lee H, Son SY, Lee CH., Kim SY, Lim Y. Ameliorative Effect of *Annona muricata* (Graviola) Extract on Hyperglycemia Induced Hepatic Damage in Type 2 Diabetic Mice. *Antioxidants*, 2021, 10(10), Article 10. <https://doi.org/10.3390/antiox10101546>
37. Forouzesh N, Onufriev AV. MMGB/SA Consensus Estimate of the Binding Free Energy Between the Novel Coronavirus Spike Protein to the Human ACE2 Receptor. *BioRxiv*, 2020.08.25.267625. 2020, <https://doi.org/10.1101/2020.08.25.267625>
38. Akinnusi PA, Olubode SO, Alade AA, Ahmed SA, Ayekolu SF, Ogunlade TM, Gbore DJ, Rotimi OD, Ayodele AO. A molecular modeling approach for structure-based virtual screening and identification of novel anti-hypercholesterolemic agents from Grape. *Informatics in Medicine Unlocked*, 2022, 32, 101065. <https://doi.org/10.1016/j.imu.2022.101065>
39. Bondock S, Albarqi T, Shaaban I, Abdou M. Novel asymmetrical azines appending 1,3,4-thiadiazole sulfonamide: Synthesis, molecular structure analyses, in silico ADME, and cytotoxic effect. *RSC Advances*, 2023, 13(15), 10353–10366. <https://doi.org/10.1039/D3RA00123G>
40. Amin L. P-glycoprotein Inhibition for Optimal Drug Delivery. *Drug Target Insights*, 2013, 7, 27–34. <https://doi.org/10.4137/DTI.S12519>
41. Finch A, Pillans P. P-glycoprotein and its role in drug-drug interactions. 2014, <https://doi.org/10.18773/austprescr.2014.050>
42. Qi D, Dou Y, Zhang W, Wang M, Li Y, Zhang M, Qin J, Cao J, Fang D, Ma J, Yang W, Xie S, Sun H. The influence of verapamil on the pharmacokinetics of the pan-HER tyrosine kinase inhibitor neratinib in rats: The role of P-glycoprotein-mediated efflux. *Investigational New Drugs*, 2023, 41(1), 13–24. <https://doi.org/10.1007/s10637-022-01314-7>
43. Stalinska J, Zimolag E, Pianovich NA, Zapata A, Lassak A, Rak M, Dean M, Ucar-Bilyeu D, Wyczechowska D, Culicchia F, Marrero L, Del Valle L, Sarkaria J, Peruzzi F, Jursic B, Reiss K. Chemically Modified Variants of Fenofibrate with Antiglioblastoma Potential. *Translational Oncology*, 2019, 12(7), 895–907. <https://doi.org/10.1016/j.tranon.2019.04.006>
44. Pardridge WM. Drug transport across the blood–brain barrier. *Journal of Cerebral Blood Flow & Metabolism*, 2012, 32(11), 1959–1972. <https://doi.org/10.1038/jcbfm.2012.126>
45. Pimentel E, Sivalingam K, Doke M, Samikkannu T. Effects of Drugs of Abuse on the Blood-Brain Barrier: A Brief Overview. *Frontiers in Neuroscience*, 2020, 14, 513. <https://doi.org/10.3389/fnins.2020.00513>
46. Leclerc M, Dudonné S, Calon F. Can Natural Products Exert Neuroprotection without Crossing the Blood–Brain Barrier? *International Journal of Molecular Sciences*, 2021, 22(7), Article 7. <https://doi.org/10.3390/ijms22073356>
47. Wu D, Chen Q, Chen X, Han F, Chen Z, Wang Y. The blood–brain barrier: Structure, regulation, and drug delivery. *Signal Transduction and Targeted Therapy*, 2023, 8(1), Article 1. <https://doi.org/10.1038/s41392-023-01481-w>
48. Lynch T, Price A. The Effect of Cytochrome P450 Metabolism on Drug Response, Interactions, and Adverse Effects. *American Family Physician*, 2007, 76(3), 391–396. <https://www.aafp.org/pubs/afp/issues/2007/0801/p391.html>
49. Deodhar M, Al Rihani SB, Arwood MJ, Darakjian L, Dow P, Turgeon J, Michaud V. Mechanisms of CYP450 Inhibition: Understanding Drug-Drug Interactions Due to Mechanism-Based Inhibition in Clinical Practice. *Pharmaceutics*, 2020, 12(9), 846. <https://doi.org/10.3390/pharmaceutics12090846>
50. Guengerich FP. A history of the roles of cytochrome P450 enzymes in the toxicity of drugs. *Toxicological Research*, 2021, 37(1), 1–23. <https://doi.org/10.1007/s43188-020-00056-z>
51. Lipinski CA, Lombardo F, Dominy BW, Feeney PJ. Experimental and computational approaches to estimate solubility and permeability in drug discovery and development settings. *Advanced Drug Delivery Reviews*, 2001, 46(1–3), 3–26. [https://doi.org/10.1016/s0169-409x\(00\)00129-0](https://doi.org/10.1016/s0169-409x(00)00129-0)
52. Protti ÍF, Rodrigues DR, Fonseca SK, Alves RJ, de Oliveira RB, Maltarollo VG. Do Drug-likeness Rules Apply to Oral

- Prodrugs? ChemMedChem, 2021, 16(9), 1446–1456. <https://doi.org/10.1002/cmdc.202000805>
53. Sahu VK, Singh RK, Singh PP. Extended Rule of Five and Prediction of Biological Activity of Peptidic HIV-1-PR Inhibitors. Universal Journal of Pharmacy and Pharmacology, 2022, 20–42. <https://www.scipublications.com/journal/index.php/ujpp/article/view/403>
  54. Clark DE. Rapid calculation of polar molecular surface area and its application to the prediction of transport phenomena. 1. Prediction of intestinal absorption. Journal of Pharmaceutical Sciences, 1999, 88(8), 807–814. <https://doi.org/10.1021/js9804011>
  55. Pajouhesh H, Lenz GR. Medicinal Chemical Properties of Successful Central Nervous System Drugs. NeuroRx, 2005, 2(4), 541–553.
  56. Martin YC. A Bioavailability Score. Journal of Medicinal Chemistry, 2005, 48(9), 3164–3170. <https://doi.org/10.1021/jm0492002>
  57. Bonovas S, Nikolopoulos GK, Bagos PG. Use of Fibrates and Cancer Risk: A Systematic Review and Meta-Analysis of 17 Long-Term Randomized Placebo-Controlled Trials. PLoS ONE, 2012, 7(9), e45259. <https://doi.org/10.1371/journal.pone.0045259>
  58. Lian X, Wang G, Zhou H, Zheng Z, Fu Y, Cai L. Anticancer Properties of Fenofibrate: A Repurposing Use. Journal of Cancer, 2018, 9(9), 1527–1537. <https://doi.org/10.7150/jca.24488>
  59. Morris-Schaffer K, McCoy MJ. A Review of the LD50 and Its Current Role in Hazard Communication. ACS Chemical Health and Safety, 2021, 28(1), 25–33. <https://doi.org/10.1021/acs.chas.0c00096>
  60. Arulanandam CD, Hwang JS, Rathinam AJ, Dahms HU. Evaluating different web applications to assess the toxicity of plasticizers. Scientific Reports, 2022, 12(1), Article 1. <https://doi.org/10.1038/s41598-022-18327-0>
  61. Pallarés N, Barba F, Berrada H, Tolosa J, Ferrer E. Pulsed Electric Fields (PEF) to Mitigate Emerging Mycotoxins in Juices and Smoothies. Applied Sciences, 2020, 10, 6989. <https://doi.org/10.3390/app10196989>
  62. Scheler S, Fahr A, Liu X. Linear combination methods for prediction of drug skin permeation. ADMET and DMPK, 2014, 2(4), 4. <https://doi.org/10.5599/admet.2.4.147>
  63. Yadav AR, Mohite SK. ADME Analysis of Phytochemical Constituents of Psidium guajava. Asian Journal of Research in Chemistry, 2020, 13(5), 373–375. <https://doi.org/10.5958/0974-4150.2020.00070.X>

#### HOW TO CITE THIS ARTICLE

Zacchaeus SO, Labunmi L, Olayinka FO, John CE, Bessie ET, Gabriel OO, Olaniyi OI, Olawumi TO, Anikeola CO. Exploration of Secondary Metabolites in Flower-Petal *Annona muricata* as Agonists for Peroxisome Proliferator-Activated Receptor-Alpha (PPAR $\alpha$ ) for Liver Function. J Phytopharmacol 2023; 12(6):411-420. doi: 10.31254/phyto.2023.12607

#### Creative Commons (CC) License-

This article is an open access article distributed under the terms and conditions of the Creative Commons Attribution (CC BY 4.0) license. This license permits unrestricted use, distribution, and reproduction in any medium, provided the original author and source are credited. (<http://creativecommons.org/licenses/by/4.0/>).